Nuclear spin conversion in the gaseous phase in the presence of a static electric field: Intramolecular magnetic interactions and the role of collisions

P. Cacciani,* J. Cosléou, F. Herlemont, M. Khelkhal, and J. Lecointre
Laboratoire de Physique des Lasers, Atomes et Molécules, CERLA, Centre Lasers et Applications, Université des Sciences et Technologies de Lille, 59655 Villeneuve d'Ascq Cedex, France
(Received 17 October 2003; published 16 March 2004)

When a gaseous sample of $^{13}CH_3F$ is prepared with a spin-isomer population ratio (ortho and para forms) far from the equilibrium given by nuclear spin statistics, it relaxes towards this equilibrium with an exponential decay rate. This phenomenon, called nuclear spin conversion, is mainly governed by intramolecular spin-spin and spin-rotation interactions which couple two pairs of quasidegenerate ortho-para levels ($J=9,K=3$; $J'=11,K'=1$) and ($J=20,K=3$; $J'=21,K'=1$). The presence of a static electric field can induce the degeneracy for Stark sublevels and yields an increase of the conversion rate. Such a "conversion spectrum" has been recorded experimentally. The intensities of the peaks are directly related to the intramolecular magnetic interaction strengths, and their widths depend on how the collisions break the coherence between ortho and para levels which is created by the interactions. Such collision-induced rates are directly determined and compared to the rate of rotationally inelastic molecular collisions.

DOI: 10.1103/PhysRevA.69.032704 PACS number(s): 34.30.+h, 31.30.Gs, 34.90.+q

I. INTRODUCTION

The $^{13}CH_3F$ molecule has two spin isomers: "ortho" with parallel nuclear spins of the three hydrogen atoms ($I=3/2$) and "para" when one of the hydrogen nuclear spins is flipped ($I=1/2$). In the gaseous phase, these isomers are not so stable as for the hydrogen molecule and they can convert one into the other with a nuclear spin conversion rate determined by previous experiments as $\gamma=12.2(6)\times10^{-3}$ s^{-1}/Torr [1–4]. A theoretical approach to this nuclear spin relaxation was proposed in 1967 by Curl *et al.* [5] and developed in 1991 by Chapovsky [6] with the help of a density matrix formalism. To change the total nuclear spin of a molecule, a magnetic field gradient is needed on the molecular scale. Intramolecular magnetic interactions like spin-spin or spin-rotation, which are responsible for the hyperfine structure, are good candidates. These weak interactions are efficient only if there exists some degeneracy of rotational states with different spin symmetries. In such conditions, the quantum states are no longer pure para or ortho states but are mixed states. These mixings play the role of gates between ortho and para subspaces. Because of the rotational relaxation, a molecule initially in ortho subspace can reach one of these gate levels and then its wave function is described by a mixing of ortho and para components. The next inelastic collision will transfer out the molecule of this mixed state, with some nonzero probability to end up in the para subspace.

For $^{13}CH_3F$, spectroscopic studies have specified the available pairs of levels in the vibrational ground state which are significantly coupled by intramolecular interactions. The role of two of these pairs has been illustrated in our recent experiment where a triangular alternating electric field was applied [7]. As the electric field amplitude increases, the Stark sublevels of the first pair ($J=9,K=3$; $J'=11,K'=1$), coupled by spin-spin interactions only, start to cross (around 600 V/cm) and the increase in the conversion rate allows an interaction strength measurement. A second increase (around 4000 V/cm) occurs when the Stark levels of the second pair ($J=20,K=3$; $J'=21,K'=1$) cross. For this last pair, both spin-spin and spin-rotation interactions are involved and, for the first time, information on spin-rotation could be derived from observations [7].

Theoretically, the presence of an external electric field is taken into account by considering, instead of a sole pair of ortho-para levels, the contribution of all pairs of Stark sublevels, with the corresponding possible degeneracies. Experimentally, the application of an alternating triangular electric field allows one to extract the interaction terms whatever the relaxation of the coherence rate $\Gamma_{\alpha,\alpha'}$ is [7]. These rates were introduced in the nuclear spin conversion model as phenomenological parameters which describe how the coherence of the mixed state is destroyed by the collisions. They have never been experimentally measured and, in previous studies [1–4], their values were taken equal to those of the population relaxation rates. In our scheme, we propose to measure the conversion rates in a static electric field in order to have access both to the interaction strengths and to the relaxation rates $\Gamma_{\alpha,\alpha'}$.

The paper is organized as follows: Section II presents the results of the "quantum relaxation" model in the case of a static electric field. Section III describes the experimental setup and the processes used to measure all parameters which are needed to derive the conversion rates. Section IV presents the experimental results. Then, in Sec. V, we analyze these results in the frame of the quantum relaxation model and we discuss the derived interaction strengths and relaxation rates.

II. THEORETICAL BACKGROUND

The calculation of the conversion rate versus the electric field can be done by extending the model of "quantum" re-

*Electronic address: Patrice.Cacciani@univ-lille1.fr

laxation [6]. As this model has been presented in previous publications, we will just give in this paper what is necessary to discuss our results.

In such a model, the quantitative description of the conversion process is given by the relaxation of the nonequilibrium concentration of, e.g., ortho molecules. The excess of ortho molecules $\delta\rho_0(0)$, created at time $t=0$, decays exponentially:

$$\delta\rho_0(t) = \delta\rho_0(0)e^{-\gamma t}. \tag{1}$$

The rate γ is expressed as [6]

$$\gamma = \sum_{\substack{\alpha\in ortho \\ \alpha'\in para}} \frac{2\Gamma_{\alpha\alpha'}|V_{\alpha\alpha'}|^2}{\Gamma_{\alpha\alpha'}^2+\omega_{\alpha\alpha'}^2}[W_B(\alpha)+W_B(\alpha')]. \tag{2}$$

The summation is made over all ortho α and para α' level pairs, $V_{\alpha\alpha'}$ is the matrix element of the interaction expressed in $\hbar$ units, W_B is the Boltzmann factor, $\hbar\omega_{\alpha\alpha'}$ is the energy difference between the levels of the pair, and $\Gamma_{\alpha\alpha'}$ is the collisional decay rate of the coherence which is the off-diagonal element of the density matrix $\rho_{\alpha\alpha'}$. The validity of this model holds with the assumption that the interaction strength $V_{\alpha\alpha'}$ remains small compared to the pair energy difference $\omega_{\alpha\alpha'}$ or to the relaxation rate of the coherence $\Gamma_{\alpha\alpha'}$ [9].

In the absence of an electric field, the spin conversion rate is dominated by the occurrence of quasidegenerate ortho-para pairs in the molecule. As the values of the corresponding energy gaps have been determined by the spectroscopy, the dependence relies then only on the magnetic interaction strengths $V_{\alpha\alpha'}$ (spin-spin and spin-rotation) and on the $\Gamma_{\alpha\alpha'}$ parameters.

Analysis of the conversion in an electric field gives the opportunity to measure independently these parameters. In our previous paper [7], we demonstrated the possibility of removing the $\Gamma_{\alpha\alpha'}$ dependence by using an alternating triangular electric field. Applying a well-calibrated static electric field allows one to measure the whole set of parameters.

When an electric field F is applied, formula (2) still holds if we replace in the sum each $(\alpha\alpha')$ pair by the $(2J+1)(2J'+1)$ Stark sublevels pairs. The energy difference is then given by

$$\hbar\omega_{\alpha M,\alpha' M'} = \hbar\omega_{\alpha\alpha'} - F\mu\left(\frac{MK}{J(J+1)} - \frac{M'K'}{J'(J'+1)}\right), \tag{3}$$

with the possibility that this value could be zero for some peculiar electric field strengths corresponding to the crossing of M sublevels. Since the Stark energy is considered low compared to the rotational one, the Boltzmann factor is equally spread over the M sublevels. M-selection rules are now considered for the magnetic interaction terms $V_{\alpha\alpha'}$ which are replaced by $V_{\alpha M,\alpha' M'}$ [8]. Both spin-spin and spin-rotation terms have to be considered; it follows that

$$|V_{\alpha M,\alpha' M'}|^2 = |V_{\alpha M,\alpha' M'}^{spin\text{-}spin}|^2 + |V_{\alpha M,\alpha' M'}^{spin\text{-}rotation}|^2. \tag{4}$$

Since the two pairs involved for $^{13}CH_3F$ have both $|\Delta K|=2$, the interaction term only involves two parameters: the spherical component of the spin-spin interaction second-rank tensor $\mathcal{T}_{22}$ and the spherical component of the spin-rotation tensor C_{22}.

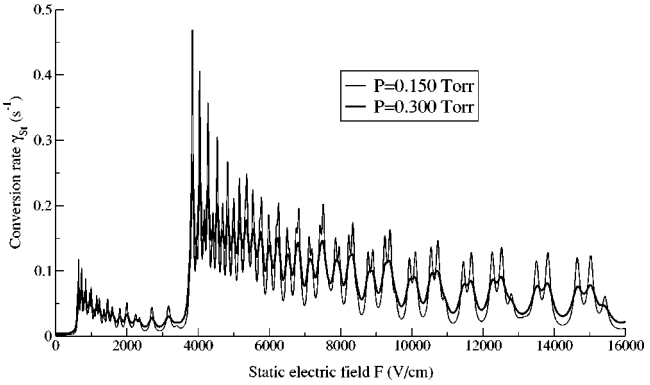

FIG. 1. Dependence of the nuclear spin conversion rate in the presence of a static electric field. The calculation is done for two pressures $P=0.150$ Torr and $P=0.300$ Torr to illustrate the pressure dependence via $\Gamma_{\alpha,\alpha'}$.

Improving the hypothesis where the same $\Gamma_{\alpha,\alpha'}$ was considered for both pairs [6,9], $\Gamma_{\alpha\alpha'}$ is supposed to be dependent on the pair through the rotational quantum numbers (J,J'), but remains independent of the (M,M') Stark sublevels.

Equation (2) becomes, in the presence of a static field,

$$\gamma_{St} = \sum_{\substack{\alpha,M \\ \alpha',M'}} \frac{2\Gamma_{\alpha\alpha'}|V_{\alpha M,\alpha' M'}|^2}{\Gamma_{\alpha\alpha'}^2+(\omega_{\alpha M,\alpha' M'})^2}(W_\alpha + W_{\alpha'}). \tag{5}$$

To illustrate this formula, we have calculated for two pressures ($P=0.150$ Torr and $P=0.300$ Torr, 1 Torr $=133$ Pa) the dependence of the conversion rate versus the electric field. The set of parameters is the one selected from our previous paper [7] obtained in a triangular electric field: $\Gamma_{11,1;9,3}=\Gamma_1=1.03\times10^8$ s^{-1}/Torr^{-1}, $\Gamma_{21,1;20,3}=\Gamma_2=0.94\times10^8$ s^{-1}/Torr^{-1}, $\mathcal{T}_{22}=77$ kHz, and $C_{22}=1.52$ kHz. The curves are plotted in Fig. 1.

III. EXPERIMENTAL SETUP AND FEATURES

The experimental setup has been described in previous publications [7,10–12].

After an enrichment of the sample by light-induced drift (LID) [1], relaxation towards spin statistics equilibrium is observed by comparing the differential absorption of the ortho species between two cells: a reference cell at equilibrium and a "conversion" cell connected to the end of a drift tube where the enrichment is made. The laser beam is split and modulated by a chopper at the frequency of 200 Hz. The two beams enter alternatively the two cells and are then combined on a pyroelectric detector. Without enrichment, the laser beams after the cells have the same intensity and the detector collects a constant power, resulting in a zero signal. Enrichment and conversion is observed via the disequilibrium between the two arms of the system.

The geometry of the cells has been described previously in [7] as well as the specific temporal scheme which has been

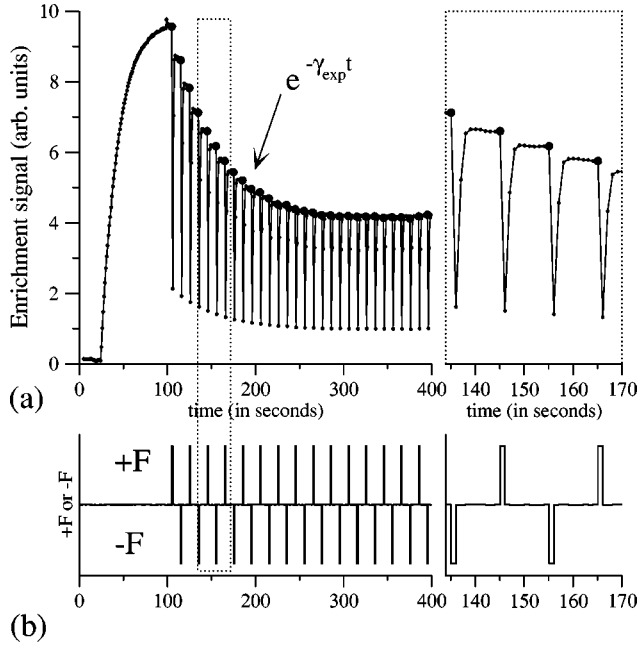

FIG. 2. Typical recording of the conversion rate in the presence of an electric field: (a) enrichment signal, (b) applied electric field, the electric field being alternatively positive and negative. Large dots are used to derive the exponential decrease γ_{exp}. An enlargement is shown on the right of the figure: the large points are taken close to the end of the period without a field.

designed to allow conversion rate measurement in the presence of an electric field. Briefly, the probe beam goes through the conversion cell between the electrodes where the field is applied. As the levels split into their Stark components, the absorption changes and can no longer be ortho or para selective. Thus the detection becomes inefficient when an electric field is applied. So the time schedule has been modified to keep an efficient detection while applying large electric fields. The field is applied only on the test cell for a certain duration T_{St}, during which the conversion rate γ_{St} takes place. Then, the field is set to zero during another time T_0 to measure the ortho enrichment with an efficient detection. During this time T_0, the conversion rate is γ_0. We chose a reference period of $T_{tot}=T_0+T_{St}=10$ s, which can be split differently depending on the conversion rate to measure. The signal is recorded every second, but we select only one significant point every 10 s; it is chosen at the end of the period without a field. As the signal is delivered by a lock-in amplifier with a 300-ms time constant, T_0 is kept greater than 3 s, giving enough time for the signal to recover. During the T_{St} period, the differential absorption becomes very large and overloads the amplifier. To avoid this, the signal is gated during the period without a field.

An example of a recording for a voltage of 314.45 V is shown in Fig. 2. This value corresponds to an electric field of 3813 V/cm for which the Stark sublevels of the second pair nearly cross. The conversion rate was expected quite high (>0.1 s^{-1}), so we have chosen the following time duty cycle $(T_{St},T_0)=(1\text{ s},9\text{ s})$. On the right part, the time scale is enlarged to show the time schedule and the recorded data points. The extraction of the conversion rate γ_{exp} is performed with the large dots, which lie close to the end of the zero-field period of 9 s.

The analysis of the exponential decrease versus time is done using these significant points and results in a derivation of the rate γ_{exp}. This rate contains two kinds of averages: (i) the temporal one considering the period with and without a field, and (ii) a volume one between the volume V_{St} (between the electrodes) and a dead volume V_0 (connexion to the drift tube) with no electric field. As has been shown previously [7], two parameters $\eta=V_{St}/(V_0+V_{St})$ and $\beta=T_{St}/(T_0+T_{St})$, which represent the ratio "with a field" in volume and in time, respectively, allow one to connect the measured γ_{exp} to the conversion rate in the absence (γ_0) or presence (γ_{St}) of the field:

$$\gamma_{exp}=\eta\beta\gamma_{St}+(1-\eta\beta)\gamma_0. \tag{6}$$

To evaluate the volume $V_{cell}=V_0+V_{St}$ of the enriched cell, we use the ability of pressure measurements given by a MKS Baratron gauge and compare the volume V_{cell} to a reference volume. The only way to access V_{St} is to measure the geometry of the cell—i.e., the surface of the electrodes and the spacing between them. The values are $V_{cell}=1.643(60)$ cm^3 and $V_{St}=10.90(10)\times d$(cm) cm^3 where d is the electrode spacing. Uncertainty in the volume determination results in an uncertainty in deriving γ_{St} from the measured γ_{exp}. Therefore, for this experiment, we have built a new cell with extreme care on the homogeneity of the electric field. A calibration has been performed by scanning the infrared Stark spectrum of the $Q(1,1)$ and $Q(2,2)$ transitions in the ν_3 band of $^{12}CH_3F$ with $9P(18)$ CO_2 laser emission. The resonant voltages were divided by the resonant field strengths measured by Freund *et al.* [13] around 4 and 12 kV/cm, respectively. The ratio is the same for both sets of transitions, ensuring the linearity of the voltage measurement. If this is assumed to give an absolute value, we derive a spacing between the electrodes of $d=0.082\,46(5)$ cm, close to the spacer size of 0.0807 cm. The line-shape analysis of the recorded spectrum gives a maximum value of 5×10^{-3} for the inhomogeneity created by a possible nonparallelism between the electrodes. This calibration procedure ensures knowledge of the electric field with a relative accuracy of 7×10^{-4}.

This value of the spacing gives $V_{St}=0.8988(91)$ cm^3 and $\eta=0.546(26)$.

It can be noticed that the conversion phenomenon is more demanding than a Stark spectroscopy experiment as regards the homogeneity: in this latter case, one has to know the field only for molecules located in the laser beam, whereas for the conversion rate measurements, one has to know the field applied for every molecule present in the cell. In our hypothesis, we assume that the electric field is strictly zero for the volume V_0 of the tube connecting the valve. More realistically, we should have to consider that a small amount of molecules are submitted to all intermediate electric fields between zero and the field strength applied between the electrodes. For this purpose, formula (6) was replaced by an integration over the total cell volume. In particular, this allows us to include fringe effects near the end of the electrodes.

Further care is taken to avoid any cumulative storing of electric charges on the glass parts of the cell. The electric field is applied alternatively positive and negative each T_{tot} period, ensuring that the time average voltage is zero. The drawback is that the positive and negative absolute values of the voltage are not rigorously the same because of a small asymmetry of the amplifier gain. A relative difference of 2×10^{-3} of the electric field strength has been measured, which has been taken into account.

IV. RESULTS

We have performed more than 400 measurements of the conversion rate at different pressures and electric field strengths.

In the model, we have considered collisions between molecules within the gas sample, but collisions of molecules with the surface of the cell have also to be considered [1,4]. This gives a constant contribution when the pressure is varied, whereas the volume contribution increases linearly. In order to determine this wall contribution for our cell, we have performed and analyzed conversion rate measurements without a field for different pressures. From these results, we separate the gas phase contribution from the wall surface one:

$$\gamma_{exp} = \gamma_{wall} + \gamma_0^P P, \tag{7}$$

$$\gamma_{exp}(\mathrm{s}^{-1}) = 1.17(40)\times10^{-3} + 11.7(15)\times10^{-3}\ P, \tag{8}$$

where the pressure is given in Torr. This value is in agreement with the previous measurements $\gamma^P = 12.2(6)\times10^{-3}\ \mathrm{s}^{-1}/\mathrm{Torr}$ [1–4].

From the volumes $(V_{cell}, V_0, V_{St}, \eta)$ and time schedule $(T_{St}, T_0, T_{tot}, \beta)$, we can derive the gas phase conversion rate γ_{St} at the specific electric field value F from the apparent conversion rate γ_{exp}. We assume in our model that the wall contribution remains the same in the presence of the electric field.

For the measurements with an electric field, the evolution of the relaxation rate can be observed in two different ways: (i) versus the Stark field for a fixed pressure and (ii) versus pressure at fixed field strength. In this last case, we have chosen the Stark field strength corresponding to a crossing.

For the first kind of investigation, the pressure was fixed at 0.180 Torr; seven crossings were probed for the first pair of ortho-para levels and eight for the second pair (Fig. 3). Figures 4 and 5 show enlargements around the field strengths $F=3500$ V/cm and 15 000 V/cm. The M,M' values and the corresponding field strength at the crossing are summarized in Table I. The pressure was chosen as low as possible to have narrow peaks for the determination of the relaxation rates Γ_1 and Γ_2, with the limit of keeping a good enrichment and conversion signal for the accuracy of the conversion rate measurement.

The two first main crossings of each pair have been studied also at a higher pressure of $P=0.260$ Torr in order to study the broadening described by the linear dependence of Γ_1 and Γ_2 versus the pressure. This is illustrated in Fig. 6.

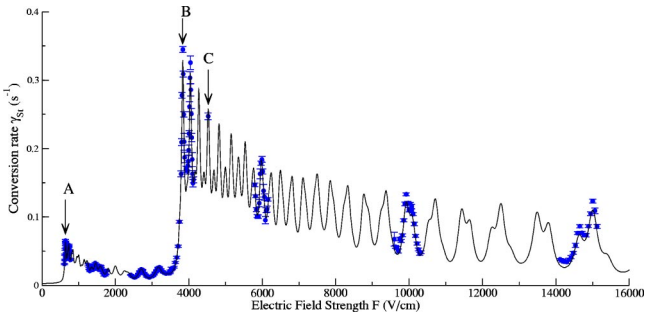

FIG. 3. Experimentation data for a pressure of 0.180 Torr for different electric field strengths around Stark sublevel crossing values. The plain curve represents the calculation with the quantum relaxation model parameters fitted on the experimental data points. The three arrows labeled A, B, and C represent the field strengths where a study has been performed at fixed field by varying the pressure.

To complete the study of pressure dependence, we have measured the conversion rates for three fixed field values (646.8 V/cm, 3838 V/cm, 4529.1 V/cm) at the maxima of peaks, the pressure being varied from 0.120 to 0.500 Torr. These fields are labeled by A, B, and C in Table I and appear with an arrow in Fig. 3. The agreement between the data and the calculated rates with fitted parameters is shown on Fig. 7. For these maxima, we are exactly at the crossing point for one specified ortho and para Stark level pair; the conversion rate decreases with increasing pressure, which represents an increase in the number of collisions. This behavior has been already described by Nagels *et al.* [14] and interpreted in term of a quantum Zeno effect. Besides formula (5) derived from the quantum relaxation model, a microscopical explanation can be given. Suppose that a molecule, initially in the ortho subspace, arrives at $t=0$ by collision in an ortho Stark

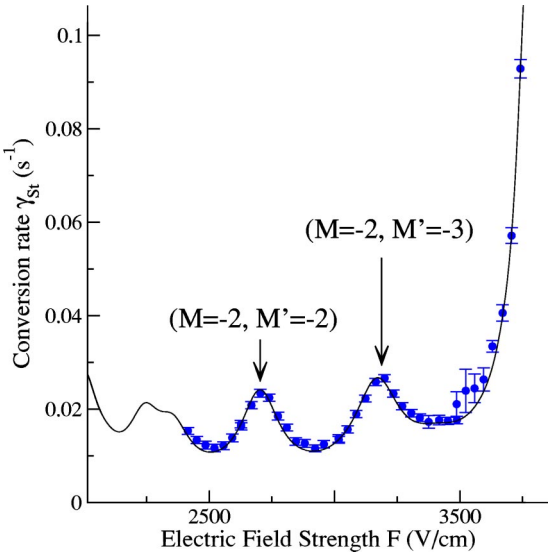

FIG. 4. Conversion "spectrum" at $P=0.180$ Torr for the crossings $(M=-2, M'=-2)$ and $(M=-2, M'=-3)$ of the first pair. The large increase on the right is the first main crossing of the second pair with $M=20, M'=21$. Calculated curves are drawn with the fitted parameters of the study.

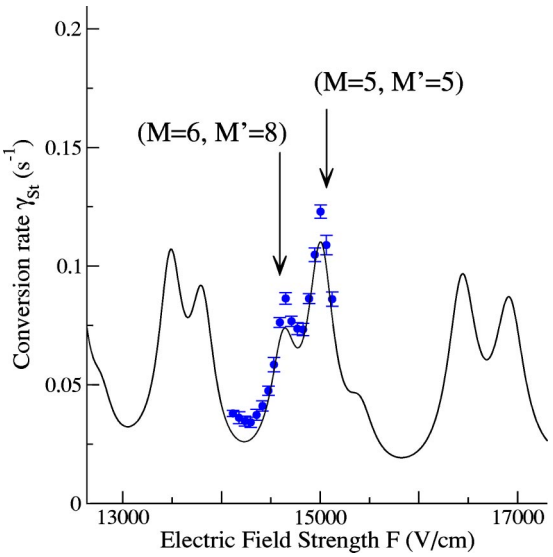

FIG. 5. Conversion "spectrum" at $P=0.180$ Torr for the crossings $(M=6,M'=8)$ and $(M=5,M'=5)$ of the second pair.

sublevel which is degenerate with its para partner. At this specific crossing point, the ortho and para states are strongly mixed (which differs from the zero-field case). The wave function has an oscillatory behavior at a frequency given by $\Omega=V$. This frequency is low compared to $\Gamma_{\alpha,\alpha'}$, and by increasing the pressure, the molecule has less and less time between two collisions to start the oscillation during which the para character will be gained and, so, to have a probability of conversion. This explains that, near a specific crossing, the conversion rate is roughly proportional to the inverse of the pressure.

All the data have been treated by a weighted least-squares-fit procedure following the model described by Eq. (5). Each data point is considered with its corresponding pressure and electric field, and the weight is derived from the uncertainty in the conversion rate given by the exponentially decreasing fit. The fitted parameters are the interactions strengths T_{22} and C_{22} (spin-spin and spin-rotation) and the relaxation rates of the ortho-para coherence created by the magnetic interactions Γ_1 and Γ_2. As mentioned in Sec. II, we have made the assumption that the relaxation rate depends only on the considered pair and not on the (M,M') Stark sublevels. This hypothesis will be discussed later.

In fact, a fifth parameter was required in order to be able to adjust the electric field position of the conversion rate maxima. In the model, a constant dipole moment $\mu_0=1.8579(6)$D [13] was first used. But despite accurate calibration of the field and spectroscopic efforts on the knowledge of the zero-field energy differences $\omega_{\alpha,\alpha'}$ [130.35(18) MHz for the first pair and 351.40(43) MHz for the second pair], a significant shift in electric field strength subsisted between calculated and experimental points especially for the crossings corresponding to the second pair.

TABLE I. Crossings studied.

M	M'	Electric field (V/cm)	
	$J=9,\ K=3;\ J'=11,\ K'=1$		
−9	−11	643.00[a]	(A)
−8	−10	729.76[a]	
−4	−4	1352.1[a]	
−4	−5	1459.5[a]	
−4	−6	1585.4[a]	
−2	−2	2704.3[a]	
−2	−3	3170.8[a]	
	$J=20,\ K=3;\ J'=21,\ K'=1$		
20	21	3845.8	(B)
19	20	4052.9	
17	18	4542.3	(C)
13	14	5988.3	
8	9	9946.3	
7	6	10120.0	
6	8	14667.0[a]	
5	5	15048.0	

[a]Spin-spin only.

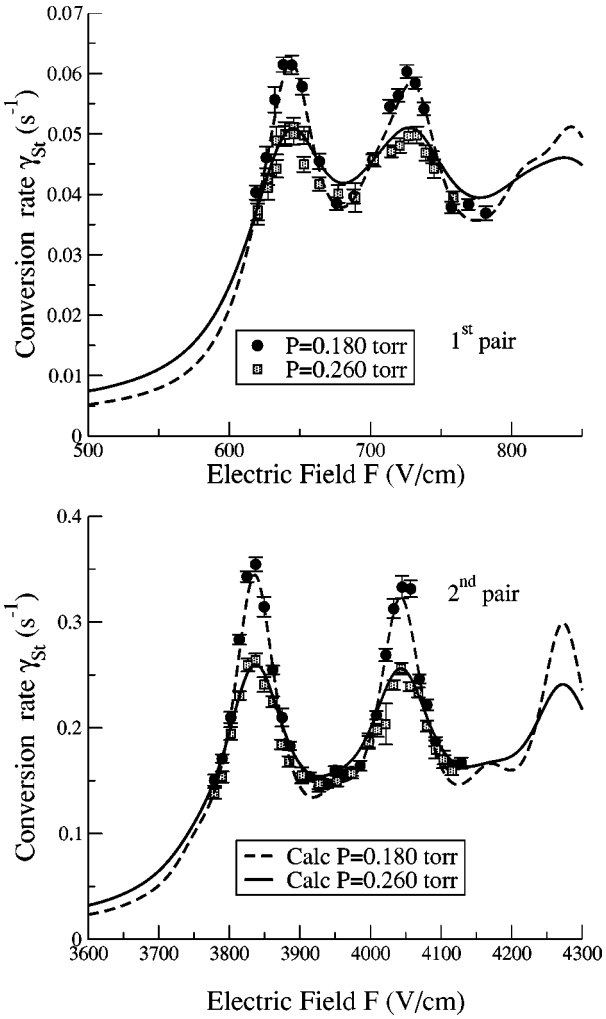

FIG. 6. Conversion "spectrum" around the two first Stark crossings for the first and second pairs: dependence vs Stark field for two pressures $P=0.180$ Torr and $P=0.260$ Torr. Calculated curves are drawn using the fitted parameters of the study (see text).

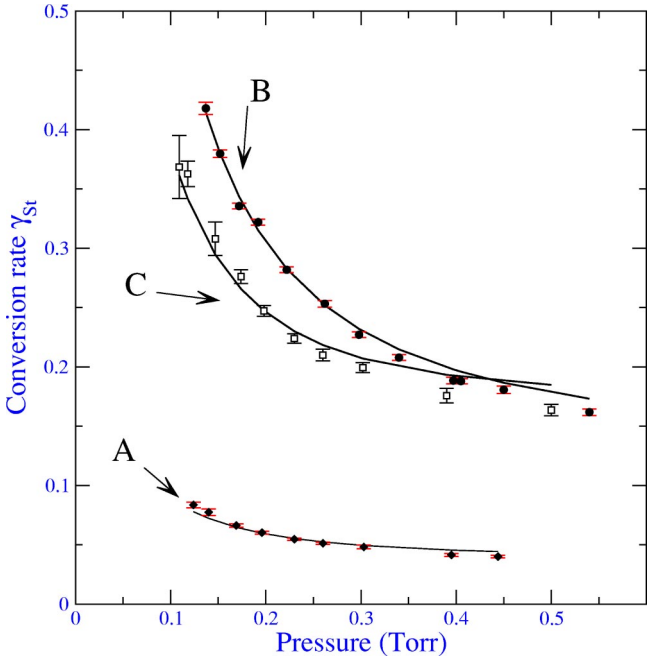

FIG. 7. Conversion rate dependence vs pressure for three maxima of the conversion "spectrum" labeled A, B, and C (see Fig. 3).

Then, considering the high J values of the involved levels, we introduced a rotational dependence of the dipole moment $\mu=\mu_0+\mu_J J(J+1)+\mu_K K^2$. Here μ_J is considered as a fifth parameter, assuming μ_K fixed at a constant value -3.7×10^{-5} D [15]. This aspect will be detailed elsewhere [16].

The best adjusted parameters are summarized in Table II. An example of the agreement can be seen in Fig. 3 where the curve is calculated for a pressure of 0.180 Torr. The good agreement is also visible in Fig. 7 where the calculation is done at fixed field strength versus pressure.

The quality of the overall fit is given by the value of the reduced $\chi^2=3.8$.

V. DISCUSSION

The agreement between experiment and theory confirms the validity of the "quantum" relaxation model and its adaptation in the presence of an electric field.

The fitted parameters reported in Table II are relevant to either the strength of the intramolecular interactions (T_{22},C_{22}) or the collisional relaxation rates (Γ_1,Γ_2). We will first discuss the values of intramolecular interactions and compare them to previous experiments. Second, we will focus on the role of collisions, their implication in the quantum relaxation model, and their ability to describe our experimental observations.

A. Intramolecular interactions

The value of $T_{22}=67.9$ kHz is in good agreement with the theoretical value of 69.2 kHz calculated from the molecular structure [17,18] and the previous experimental value of 69.7 kHz [12]. It corrects the one derived from experiment with a triangular alternating field of 77 kHz [7]. Compared to this approach, the two interaction strengths can be separately derived from the data; a good example is given in the highest studied crossing (Fig. 5, $F=15$ kV/cm). In the double peak, the first component $(M=6,M'=8)$ is driven only by spin-spin interactions $(\Delta M=2)$, whereas the second peak $(M=5,M'=5)$ is mainly (85%) driven by spin-rotation interactions. So the two "intensities" give directly and separately the two interaction strengths. With the triangular alternating field method, the spin-spin interaction was first derived from the increase due to the first pair; then the spin rotation interaction was estimated by subtracting the spin-spin contribution from the increase due to the second pair. So the error made in the spin-spin term was transferred to the spin-rotation one. We mentioned in the discussion in Ref. [7] that if the spin-spin term is taken at its theoretical value of 69.2 kHz, the derived value of the spin-rotation term will be 1.85 kHz. So the value of $C_{22}=1.99$ kHz found in the present work is in agreement with previous measurements.

In a theoretical work, Gus'kov [19] introduced the role of the spin-rotation interaction in the model. Considering only spin-spin interactions for the two pairs and assuming experimental values for the relaxation rates [20] of $\Gamma_1=1.09\times10^8$ s^{-1}/Torr and $\Gamma_2=1.00\times10^8$ s^{-1}/Torr, a calculated value was found to represent only 40 % of the experimental nuclear spin conversion rate in $^{13}CH_3F$. Therefore, the author assigned the remaining part to a spin-rotation interaction strength of 2.12 kHz, qualitatively compatible with our value.

B. Collisional relaxation rates

The study of the conversion spectrum was mainly focused on the ability to measure directly the relaxation rates of the

TABLE II. Best-fitted parameters. The errors in parentheses correspond to one standard deviation of the values in the least-squares-fit analysis.

Parameter	Calculated	Reference [7]	This work
T_{22}	69.2 kHz	77 kHz	67.93(25) kHz
C_{22}	2.1 kHz[a]	1.55 kHz	1.995(10) kHz
Γ_1		1.03×10^8 s^{-1}/Torr	$1.545(31)\times10^8$ s^{-1}/Torr
Γ_2		0.94×10^8 s^{-1}/Torr	$1.342(13)\times10^8$ s^{-1}/Torr
μ_J	1.50×10^{-5} D[b]		$2.7(17)\times10^{-5}$ D

[a]Derived from experimental value at zero field [19].
[b]Reference [16].

TABLE III. Self-broadening of rotational transitions. Errors are equal to one standard deviation.

$J,K \rightarrow J',K'$	Broadening 10^8 s^{-1}/Torr
$1,1 \rightarrow 2,1$	1.12(22)[a]
$0,0 \rightarrow 1,0$	1.376(19)[b]
$1,0 \rightarrow 2,0$	1.147(16)[b]
$1,1 \rightarrow 2,1$	1.146(21)[b]
$2,2 \rightarrow 3,2$	1.011(13)[b]
$5,5 \rightarrow 6,5$	0.806(10)[b]
$7,6 \rightarrow 8,6$	0.856(10)[b]
$5,5 \rightarrow 6,5$	0.806(10)[b]
$10 \rightarrow 11$	1.09(15)[c]
$20 \rightarrow 21$	1.00(6)[c]

[a]Reference [21].
[b]Reference [22].
[c]Reference [20].

ortho-para coherences Γ_1 and Γ_2 by the width of individual peaks. Our fitted values are found significantly different from Ref. [20]. In the quantum relaxation model, the relaxation rate of the coherence $\Gamma_{\alpha\alpha'}$ is introduced as a phenomenological parameter describing the breaking of the coherence $\rho_{\alpha\alpha'}$ by the collisions [6]:

$$\frac{\partial \rho_{\alpha\alpha'}}{\partial t} = -\Gamma_{\alpha\alpha'}\rho_{\alpha\alpha'} + \cdots . \tag{9}$$

In collisional relaxation, we consider collisions which remove the population incoherently from a particular state; the assumption usually made is that the coherence between two states is broken if the molecule leaves one state or the other:

$$\Gamma_{\alpha\alpha'} = \frac{\Gamma_{\alpha\alpha} + \Gamma_{\alpha'\alpha'}}{2}. \tag{10}$$

$\Gamma_{\alpha\alpha}$ and $\Gamma_{\alpha'\alpha'}$ are relaxation rates of the population α (respectively, α') which are commonly derived by studying the collisional broadening of transitions involving these states. Reference [20] is an example of such studies with rotational quantum number J but with no K resolution. Other determinations resolving the K components can be found in the literature. All are summarized in Table III.

Such an assumption of using the relaxation rates derived from collision broadening in the nuclear spin conversion model was first considered by Nagels *et al.* [23] studying the collision of $^{13}CH_3F$ with different foreign gases. This was the argument to conclude that the "quantum relaxation" model was the leading mechanism for the spin conversion in CH_3F. Recently, this interpretation was completely questioned in similar experiments performed on formaldehyde [24,25] where a nuclear spin relaxation "cross-section" was found much larger than the line broadening ones.

Beyond these questions, the hypothesis of Eq. (10) could be refined in the presence of an electric field. In the derivation of the Master equation [26], the relaxation rate of the coherence $\Gamma_{\alpha\alpha'}$ is the sum of two terms: $\Gamma_{\alpha\alpha'}^{nonadia} = \frac{1}{2}(\Gamma_{\alpha\alpha} + \Gamma_{\alpha'\alpha'})$, which corresponds to the nonadiabatic term assuming that a process that makes the molecule leaves the state α or α' necessarily breaks the coherence $\rho_{\alpha\alpha'}$, and an adiabatic one $\Gamma_{\alpha\alpha'}^{adia}$ corresponding to processes where the molecule remains in its state (α or α') but interacts with the reservoir which changes from a state μ to another state of equivalent energy ν. This last term is not effective in our case since it does not lead to nuclear conversion.

For the nonadiabatic term, in the absence of a field, the α level is degenerated in M. Efficient collisions are those which transfer the molecule from α to $\beta \neq \alpha$ corresponding to a change in the J value. The energy transfer is at least of the order of magnitude of the rotational energy. In the presence of an electric field, the M degeneracy is lifted; therefore, we have to consider, in addition to the previous ones, collisions which keep the same J values and change only M (reorientation of the molecule). The energy transfer is lower and such collisions are considered to be softer than those which contribute to the usual relaxation of the population α.

These collisions which reorient the molecule are at the origin of the phenomena of collisional coupling between Stark transitions observed on the broadening of CH_3F transitions in the presence of an electric field [27]. The main result of this study was the observation of a different collisional broadening for a transition degenerated in M in the absence of the field from the ones of individual Stark components where the electric field is strong enough to resolve them. Following the first observation of Brechignac [28], precise experimental data showed the M dependence of the collisional broadening [29,30] and how to treat overlapping Stark components [27]. The "soft" collisions which only reorient the molecule are pointed out; they can play a similar role in our nuclear spin conversion process. On purpose, we tried a least-squares fit of our data, assuming the M dependence given in [30] for Γ_1 and Γ_2. No improvement was observed.

Within the model described by Eq. (5), knowledge of $\Gamma_{\alpha,\alpha'}$ values is essential to calculate the conversion rate at zero field. Using the four parameters of Table II derived from non-zero-field conversion rate data, we found the value $\gamma^P = 15.5 \times 10^{-3}$ s^{-1}/Torr at zero field, which lies 30% higher than the commonly accepted value of $\gamma^P = 12.2(6) \times 10^{-3}$ s^{-1}/Torr. This discrepancy brings up the possibility of experimental error sources or some improvement of the model.

The fitting procedure takes into account the positive-negative disequilibrium of the electric field applied as well as some edge effects at the end of the electrodes but assumes a perfect homogeneity of the field in the Stark cell. Let us remember that lower values of Γ give more contrasted peaks that a possible inhomogeneity could smooth. Coming back to our calibration procedure of the electric field, the shape of the two Stark spectra $Q(1,1)$ and $Q(2,2)$ have been carefully examined. The observed contrast allows us to give an upper limit to the relative inhomogeneity of the field around 5×10^{-3}. Assuming such a value, we calculated its influence on the parameters of the fit: the only significant change is on the second pair where Γ_2 would be overestimated by 10%. This effect is not enough to remove the discrepancy men-

tioned above. With such a correction the conversion rate at zero field remains 20% higher than the experimentally measured one. So an improvement of the model considering, i.e., the role of the reorientating collisions has probably to be considered.

VI. CONCLUSION

Accurate measurements of the conversion rates of $^{13}CH_3F$ have been performed in the presence of a static electric field. The data are satisfactorily reproduced in the framework of the quantum relaxation model and allow us to derive separately the parameters of the model: spin-spin and spin-rotation intramolecular magnetic interactions and collisional relaxation rates. Some remaining discrepancies address the possibility of refining the model, in particular to have a better description of how the collisions break the coherence created by the magnetic interactions between ortho and para levels. The role of soft reorientational collisions is suggested as a candidate to refine the model and to improve the comparison between calculated values and experimental data.

ACKNOWLEDGMENTS

This work is part of the scientific program of the Centre d'Études et de Recherches Lasers et Applications (CERLA) which is supported by the Ministère de la Recherche, the Région Nord–Pas de Calais, and the Fonds Européen de Développement Économique des Régions.

[1] P. L. Chapovsky and L. J. F. Hermans, Annu. Rev. Phys. Chem. **50**, 315 (1999).
[2] B. Nagels, M. Schuurman, P. L. Chapovsky, and L. J. F. Hermans, Chem. Phys. Lett. **242**, 48 (1995).
[3] B. Nagels, N. Calas, D. A. Roozemond, L. J. F. Hermans, and P. L. Chapovsky, Phys. Rev. Lett. **77**, 4732 (1996).
[4] B. Nagels, Ph.D. thesis, Leiden University, The Netherlands, 1998.
[5] R. F. Curl, Jr., J. V. V. Kasper, and K. S. Pitzer, J. Chem. Phys. **46**, 3220 (1967).
[6] P. L. Chapovsky, Phys. Rev. A **43**, 3624 (1991).
[7] P. Cacciani, J. Cosléou, F. Herlemont, M. Khelkhal, and J. Legrand, Eur. Phys. J. D **22**, 199 (2003).
[8] E. Ilisca and K. Bahloul, Phys. Rev. A **57**, 4296 (1998).
[9] P. L. Chapovsky, Physica A **233**, 441 (1996).
[10] P. L. Chapovsky, J. Cosléou, F. Herlemont, M. Khelkhal, and J. Legrand, Chem. Phys. Lett. **322**, 424 (2000).
[11] J. Cosléou, F. Herlemont, M. Khelkhal, J. Legrand, and P. L. Chapovsky, Eur. Phys. J. D **10**, 99 (2000).
[12] P. Chapovsky, J. Cosléou, F. Herlemont, M. Khelkhal, and J. Legrand, Eur. Phys. J. D **12**, 297 (2000).
[13] S. M. Freund, G. Duxbury, M. Römheld, J. T. Tiedje, and T. Oka, J. Mol. Spectrosc. **52**, 38 (1974).
[14] B. Nagels, L. J. F. Hermans, and P. L. Chapovsky, Phys. Rev. Lett. **79**, 3097 (1997).
[15] K. Harada (private communication).
[16] J. Cosléou, P. Cacciani, F. Herlemont, M. Khelkhal, J. Lecointre, and P. Pracna, Phys. Chem. Chem. Phys. (to be published).
[17] J. Demaison, J. Breidung, W. Thiel, and D. Papousek, Struct. Chem. **10**, 2 (1999).
[18] T. Egawa, S. Yamamoto, M. Nakata, and K. Kuchitsu, J. Mol. Struct. **156**, 213 (1987).
[19] K. I. Gus'kov, J. Phys. B **32**, 2963 (1999).
[20] N. J. Trappeniers and E. W. A. Elenbaas-Bunschotten, Chem. Phys. Lett. **64**, 205 (1979).
[21] F. Rohart, A. Ellendt, F. Kaghat, and H. Mäder, J. Mol. Spectrosc. **185**, 222 (1997).
[22] V. Lemaire, L. Dore, G. Cazzoli, G. Buffa, O. Tarrini, and S. Belli, J. Chem. Phys. **106**, 22 (1997).
[23] B. Nagels, M. Schuurman, P. L. Chapovsky, and L. J. F. Hermans, Phys. Rev. A **54**, 2050 (1996).
[24] M. Burkart and B. Schramm, J. Mol. Spectrosc. **217**, 153 (2003).
[25] G. Peters and B. Schramm, Chem. Phys. Lett. **302**, 181 (1999).
[26] C. Cohen-Tannoudji, J. Dupont-Roc, and G. Grynberg, *Atom-Photon Interactions, Basic Processes and Applications* (Wiley, New York, 1992).
[27] V. Lemaire, L. Dore, G. Cazzoli, G. Buffa, O. Tarrini, E. Baldanzi, and S. Belli, J. Chem. Phys. **110**, 9418 (1999).
[28] P. Bréchignac J. Chem. Phys. **76**, 3389 (1982).
[29] G. Buffa, A. Di Lieto, P. Minguzzi, O. Tarrini, and M. Tonelli, Phys. Rev. A **34**, 1065 (1986).
[30] V. Lemaire, L. Dore, G. Cazzoli, G. Buffa, O. Tarrini, and S. Belli, J. Chem. Phys. **106**, 8995 (1999).